Fibre type-specific increase in passive muscle tension in spinal cord-injured subjects with spasticity

M. Charlotte Olsson[1], Martina Krüger[2], Lars-Henrik Meyer[2], Lena Ahnlund[3], Lennart Gransberg[1], Wolfgang A. Linke[2] and Lars Larsson[1,4]

Uppsala University, Department of Neuroscience, [1]Clinical Neurophysiology and [3]Rehabilitation Medicine, 75185 Uppsala, Sweden
[2]University of Münster, Physiology and Biophysics Unit, 48149 Münster, Germany
[4]Center for Development and Health Genetics, The Pennsylvania State University, University Park, PA 16802, USA

Patients with spasticity typically present with an increased muscle tone that is at least partly caused by an exaggerated stretch reflex. However, intrinsic changes in the skeletal muscles, such as altered mechanical properties of the extracellular matrix or the cytoskeleton, have been reported in response to spasticity and could contribute to hypertonia, although the underlying mechanisms are poorly understood. Here we examined the vastus lateralis muscles from spinal cord-injured patients with spasticity ($n = 7$) for their passive mechanical properties at three different levels of structural organization, in comparison to healthy controls ($n = 7$). We also assessed spasticity-related alterations in muscle protein expression and muscle ultrastructure. At the whole-muscle level *in vivo*, we observed increased passive tension (PT) in some spasticity patients particularly at long muscle lengths, unrelated to stretch reflex activation. At the single-fibre level, elevated PT was found in cells expressing fast myosin heavy chain (MyHC) isoforms, especially MyHC-IIx, but not in those expressing slow MyHC. Type IIx fibres were present in higher than normal proportions in spastic muscles, whereas type I fibres were proportionately reduced. At the level of the isolated myofibril, however, there were no differences in PT between patients and controls. The molecular size of the giant protein titin, a main contributor to PT, was unchanged in spasticity, as was the titin : MyHC ratio and the relative desmin content. Electron microscopy revealed extensive ultrastructural changes in spastic muscles, especially expanded connective tissue, but also decreased mitochondrial volume fraction and appearance of intracellular amorphous material. Results strongly suggest that the global passive muscle stiffening in spasticity patients is caused to some degree by elevated PT of the skeletal muscles themselves. We conclude that this increased PT component arises not only from extracellular matrix remodelling, but also from structural and functional adaptations inside the muscle cells, which alter their passive mechanical properties in response to spasticity in a fibre type-dependent manner.

(Resubmitted 7 July 2006; accepted after revision 21 August 2006; first published online 24 August 2006)
Corresponding authors W. A. Linke: Physiology and Biophysics Unit, University of Münster, Schlossplatz 5, D-48149 Münster, Germany; L. Larsson: Department of Neuroscience, Clinical Neurophysiology, Uppsala University, Ing 85, 3 tr., 751 85 Uppsala, Sweden. Email: wlinke@uni-muenster.de or lars.larsson@neurofys.uu.se

Spasticity is a motor disorder associated with lesions at different levels of the central nervous system due to e.g. spinal cord injury (SCI), stroke, cerebral palsy, or multiple sclerosis. Clinical syndromes are diverse, including (but not limited to) hypertonia, flexor or adductor spasms, clonus and dyssynergic patterns of contraction. Hypertonia, an abnormal increase in muscle tone, is regarded as the defining feature of spasticity having both diagnostic and therapeutic significance. The influence of exaggerated muscle stretch reflexes on muscle hypertonus (Hornby *et al.* 2006) has severe negative effects on motor performance and quality of life in patients with an upper motor neuron lesion. For many of these patients inhibition of acetylcholine release by injecting botulinum toxin into affected muscles has proven to be an efficient intervention strategy to treat this disabling condition. However, a significant number of patients with muscle hypertonia are not helped by botulinum toxin injections and there is an increasing awareness of mechanisms underlying muscle hypertonia which are unrelated to increased stretch reflex activity. Intrinsic changes in the muscle tissue itself have therefore been suggested to have a

 DOI: 10.1113/jphysiol.2006.116749

significant impact on the spastic hypertonia (Lieber *et al.* 2004).

The nature of muscle hypertonia, unrelated to stretch reflex activation, is still poorly understood. Results from the few studies published to date on intrinsic muscle properties in patients with spasticity have reported shorter muscle fibres by some (Tardieu *et al.* 1982; Fridén & Lieber, 2003), but not by others (Lieber *et al.* 2003). Passive tension (PT) was found to be increased in single fibres from spastic muscle, indicating intrinsic muscle changes unrelated to reflex activation or extracellular matrix and connective tissue (Fridén & Lieber, 2003). Surprisingly, decreased PT was observed in fibre bundles from patients with spasticity and was attributed to altered extracellular matrix material (Lieber *et al.* 2003). These apparently contradictory results warrant follow-up studies.

When resting muscles are stretched, the PT is thought to arise from several structures, including the sarcomere protein titin, the intermediate filaments, and the extracellular connective tissue located within and surrounding the muscle belly (Wang *et al.* 1991, 1993; Horowits, 1992; Granzier & Wang, 1993; Linke *et al.* 1996; Gajdosik, 2001; Neagoe *et al.* 2003; Prado *et al.* 2005). Out of these, the collagen content, cross-linking status and isoform composition, and the titin isoform expression pattern are believed to be the major determinants of PT generation (Granzier & Wang, 1993; Linke *et al.* 1996; Gajdosik, 2001; Neagoe *et al.* 2003; Prado *et al.* 2005). Titin isoform size and stiffness are highly variable among fast-twitch muscles (Prado *et al.* 2005), whereas slow muscles tend to have long titin isoforms and low titin-based stiffness (Wang *et al.* 1991; Linke *et al.* 1996; Granzier & Labeit, 2002; Prado *et al.* 2005). The relative contributions from titin and collagen to total PT vary greatly among different skeletal muscles (Prado *et al.* 2005). Mutations in titin can cause several forms of muscular dystrophy (Hackman *et al.* 2002; Lange *et al.* 2005; Udd *et al.* 2005) and secondary titin changes have also been observed in skeletal muscles from patients with Duchenne muscular dystrophy (Tkatchenko *et al.* 2001).

The purpose of this project was to unravel the mechanisms underlying intrinsic changes in the structure and function of spastic vastus lateralis muscles from patients with spinal cord injury at the protein, myofibril, muscle cell and whole muscle levels, unrelated to stretch reflex activity. To test the hypothesis that there are structural and functional changes in spasticity intrinsic to the muscle cells, we examined PT in relation to adaptations in intracellular contractile and structural proteins (myosin, titin, desmin) and the extracellular matrix. We found increased PT at the whole-muscle and single-fibre levels in spasticity, but not at the myofibrillar level. Spastic muscles contained increased proportions of fast fibres expressing myosin heavy chain (MyHC) type IIx, and only these fibres exhibited substantially elevated PT levels. The differences in PT between spastic and control muscles were unrelated to protein expression changes of titin or desmin, but are explainable by ultrastructural remodelling within both the extracellular matrix and the muscle cells.

Methods

Patient characteristics and biopsy procedures

The spasticity in the patients selected for this study was secondary to an upper motor neuron lesion at the cervical or thoracic spinal cord levels. We excluded patients with spasticity secondary to a neurodegenerative lesion, cerebral infarction or haemorrhage to obtain a more homogeneous population. Seven male SCI subjects with complete or partial para- or tetraparesis and quadriceps muscle spasticity (SCI-S) were studied (Table 1) together with seven age- and sex-matched control subjects (CTL) with no history of neuromuscular disease. The mean age for SCI-S was 44 ± 2 years (range, 38–51) and for CTL 44 ± 2 years (range, 37–52) and the SCI-S subjects were evaluated clinically prior to the experiments using the modified 5-point Ashworth scale (Table 1) (Ashworth, 1964; Bohannon & Smith, 1987; Knutsson *et al.* 1997). The percutaneous conchotome method was used under local anaesthesia to obtain biopsies from the vastus lateralis muscle with the understanding and consent of the subjects. This study was conducted in accordance with the *Declaration of Helsinki* guidelines and full written informed consent was obtained from all subjects. The study was approved by the local ethical committee at Uppsala University.

Tissue dissection

Heart and skeletal (psoas, soleus) muscle tissue was obtained from a Sprague-Dawley rat and a New Zealand White rabbit, respectively. Animals were anaesthetized and killed prior to muscle dissection according to approved guidelines of the institutional Animal Care and Use Committee (University of Münster). The tissue was stored at –80°C until usage for gel electrophoresis. A frozen tissue chunk of human soleus muscle (excised post mortem with institutional approval) was a kind gift of Professor R. Bittner (University of Vienna).

In vivo muscle function

Dynamic dynamometry was used to measure forces opposing passive movements of the knee and electromyography (EMG) was used to monitor activation patterns in stretched and shortened muscles. Passive isokinetic knee extensions and flexions were performed under the control of a dynamic dynamometer (Kin-Com

Table 1. Clinical details of spinal cord-injured subjects with spasticity

Subject	Duration (years)	Level	Severity	Spasticity (0–5)[a] Extensor	Flexor	Medicine[b]
SCI-S1	4	T8	Com	3	4	Baclofen
SCI-S2	4	C5	Incom	2	3	Baclofen
SCI-S3	16	C5	Com	1	1	Baclofen, Diazepam
SCI-S4	7	C4–C5	Incom	4	4	Baclofen, Clonazepam, Gabapentin
SCI-S5	6	C3	Incom	3	3	—
SCI-S6	17	C7–T6	Incom	4	4	Baclofen
SCI-S7	7	T11	Com	3	4	Gabapentin

Duration, duration of injury prior to examination; Level, neurological level of injury; T, thoracic and C, cervical vertebrae; Com, complete and Incom, incomplete spinal cord injury. The causes of injury included: falling tree accident, diving accident, traffic accident, ependymoma, and cavernoma. [a]Right knee extensor and flexor spasticity graded with the modified Ashworth scale as a clinical assessment of function. [b]Medicine relevant only to SCI and spasticity is listed.

H500, Chattanooga Corp., Chattanooga, TN, USA) as described previously (Knutsson *et al.* 1997). Torque and EMG in knee extensions and flexions (from 20 to 120 deg) were recorded at four different movement velocities, 15, 30, 60 and 120 deg s^{-1}. All torque recordings were corrected for gravitation. The average torque was calculated by averaging three matching records (differences $< 15\%$) from each movement type.

Muscle sample preparation

Fresh muscle biopsies were divided into two pieces. One piece was frozen in liquid nitrogen-chilled propane and stored at -80°C, and the other piece was immediately placed in an ice-cold relaxing solution (in mmol l^{-1}: 100 KCl, 20 imidazole, 7 $MgCl_2$, 2 EGTA, 4 ATP, pH 7.0; 4°C). Small bundles of ∼25–50 fibres were dissected free from the muscle and tied to a glass microcapillary tube, slightly stretched, and then placed in a skinning solution (relaxing solution containing glycerol; 50 : 50 v/v) at 4°C for 24 h. Subsequently the bundles were stored at -20°C for use within 3 weeks or treated with cryoprotectant (sucrose) solution for long-term storage at -80°C as described previously (Frontera & Larsson, 1997).

Single-fibre mechanics

A single skinned muscle fibre was dissected out from the bundle and transferred to a stainless steel experimental chamber containing pCa 9.0 solution (composition in mmol l^{-1}: 79.2 KCl, 20 imidazole, 7 EGTA, 0.02 $CaCl_2$, 5.42 $MgCl_2$, 14.5 creatine phosphate, 4.74 ATP). The ends of the fibre were securely attached to the arms of a motor (model 300H, Cambridge Technology Inc., Cambridge, MA, USA) and force transducer (model 403, Cambridge Technology) and the fibre was adjusted to an initial sarcomere length (SL) of 2.2 μm at 15°C as described previously (Moss *et al.* 1983). The chamber assembly was then placed on the stage of an inverted microscope (Olympus IX70, Tokyo, Japan) fitted with a $\times$ 40 objective and a camera (Olympus DP11). SLs were assessed from video prints (Mitsubishi P67E, Kyoto, Japan) and were taken regularly during passive force measurements in pCa 9.0 solution and during maximum activation in pCa 4.5 solution (composition in mmol l^{-1}: 64 KCl, 20 imidazole, 7 EGTA, 7.01 $CaCl_2$, 5.26 $MgCl_2$, 14.5 creatine phosphate, 4.81 ATP). Before each maximum activation, the muscle fibre was exposed to a pre-activating solution containing (in mmol l^{-1}): 79.2 KCl, 20 imidazole, 0.07 EGTA, 5.42 $MgCl_2$, 14.5 creatine phosphate, and 4.74 ATP. The ionic strength of all solutions was adjusted to 180 mmol l^{-1} using potassium hydroxide, pH 7.0 at 15°C.

For each stretch experiment, SL started at 2.2 μm with 0.2 μm SL increments until 3.8 μm. After each incremental step, stress relaxation (force decay at a constant length) was permitted for 3 min before measuring resting (passive) force in pCa 9.0, and then the solution was switched to pCa 4.5 for measurement of maximum active force. Changes in force and motor position were sampled (16-bit resolution, DAP5216a, Microstar Laboratories) at 2.0 kHz using custom-made software developed in our laboratory and data were saved to computer files for later analysis. Cross-sectional fibre area (CSA) was calculated from the fibre width at each sarcomere length, assuming a circular circumference, and maximum active tension was calculated as maximum tension developed during pCa 4.5, normalized to fibre CSA. Once mechanical measurements were finished, fibres were cut free at the points of attachment, placed in denaturing sample buffer, and stored at -80°C until subsequent analysis of MyHC isoforms.

Single myofibril mechanics

Skeletal myofibrils from SCI-S and CTL vastus lateralis muscle samples were prepared as previously described (Minajeva *et al.* 2001, 2002). Briefly, muscle tissue was thawed and skinned in ice-cold low ionic strength

buffer (in mmol l^{-1}; 75 KCl, 10 Tris, 2 $MgCl_2$, 2 EGTA, and 40 μg ml^{-1} protease inhibitor leupeptin, pH 7.1) supplemented with 0.5% Triton X-100 for a minimum of 5 h. The skinned tissue was minced and homogenized in low ionic strength buffer to separate myofibrils. Under a Zeiss Axiovert 135 microscope (Carl Zeiss, Oberkochen, Germany), a myofibril was suspended between two glass needles attached to a piezomotor (Physik-Instrumente, Karlsruhe, Germany) and a homebuilt force transducer, respectively (Minajeva *et al.* 2002). Data collection, motor control, and SL measurements were obtained with a PC, DAQ board, and custom-written LabView software (National Instruments, Austin, TX, USA). Force measurements were carried out at room temperature in relaxing buffer (in mmol l^{-1}; 8 ATP, 20 imidazole, 4 EGTA, 12 magnesium propionate, 97 potassium propionate, pH 7.0) supplemented with 40 μg ml^{-1} leupeptin. A suppressor of active force, 2,3-butanedione monoxime (BDM) (20 mmol l^{-1}), was also added to the relaxing buffer, although complete relaxation is observed in the absence of this drug as well (Linke *et al.* 1994; Mutungi & Ranatunga, 1996). The protocol consisted of stretching a myofibril stepwise from slack length by ~0.2 μm sarcomere^{-1} step^{-1}, and each step was completed in 1 s. Following each step the myofibril was held at a constant length for 20 s to wait for stress relaxation. Finally, the myofibril was released back to slack length. For analysis we considered the force at the end of the hold period, which represents titin-based force (Minajeva *et al.* 2001). Force data were related to the cross-sectional area inferred from the diameter of the specimens.

Histological analysis and electron microscopy

Frozen muscle tissue was thawed in ice-cold phosphate-buffered saline (PBS), fixed in 4% paraformaldehyde in PBS, dehydrated in an alcohol series, and embedded in Epon blocks. Semi-thin cross-sections were cut using a Reichert ultra-microtome and stained with Toluidine Blue. Images were recorded with a colour-CCD camera (Sony) under a Zeiss Axiovert 135 inverted microscope using × 5 or × 10 objectives. Fibre CSA was determined from digital images using PaintshopPro 4.12 shareware (JASC, Inc., Eden Prairie, MN, USA) by measuring the major and minor diameters of each fibre on the cross-sections and calculating the mean values for each muscle.

Contrasted thin sections were prepared for transmission electron microscopy (EM) and viewed with a Zeiss EM 900 at 80 kV (Prado *et al.* 2005). More than 200 EM images were recorded from six different SCI-S muscles and five different CTL muscles. Mitochondrial density and myofibrillar density were calculated on scanned micrographs using ImageJ software (NIH, Bethesda, MD, USA) by circling the area occupied by mitochondria/myofibrils within a rectangular region of interest and relating it to the total measured area of that region. At least five different micrographs per muscle were analysed and results averaged.

Protein isoform determination and quantification

Myosin heavy chain isoforms. These were determined by sodium dodecyl sulphate-polyacrylamide gel electrophoresis (SDS-PAGE). Each single fibre, dissolved in sample buffer, was loaded onto a 6% SDS-PAGE gel and run at 120 V for 24 h at 10°C as described previously (Larsson & Moss, 1993). Gels were subsequently silver stained and MyHC isoforms were determined.

Titin isoforms. These were detected on agarose-strengthened 2.0% polyacrylamide gels with a Laemmli buffer system, as described (Opitz *et al.* 2004; Prado *et al.* 2005). Briefly, frozen muscle was homogenized, centrifuged and solubilized. Some gel lanes were loaded with a mix of human muscle and rabbit psoas muscle expressing two titin isoforms of 3.4 and 3.3 MDa at a ratio of ~30 : 70% (Prado *et al.* 2005); the psoas bands could be used as internal standards. Alternate lanes on a gel were loaded with psoas muscle alone and human (CTL and SCI-S) muscle alone. All gels were also loaded with rabbit soleus (titin size, ~3600 kDa) and some gels with rat heart (major titin, 3000 kDa) and human soleus (titin size, 3700 kDa) to obtain additional size markers. Human soleus tissue was kindly provided by Dr R. Bittner (University of Vienna, Austria). Attempts were made to load all lanes with equal amounts of solubilized protein after spectrophotometric analysis using the Bradford method. To determine the titin : MyHC protein ratio, we used 2.8% SDS-PAGE (Minajeva *et al.* 2002). Protein bands were visualized with Coomassie Brilliant Blue and gels were digitized by multiple scanning using a CanoScan 9900F scanner. Densitometry and molecular mass measurements were performed using TotalLab software (Phoretix, Newcastle, UK). A linear relationship between log molecular mass and migration distance was assumed.

Desmin concentrations. These were quantified by the enzyme-linked immunosorbent assay (ELISA) method as previously described (Berggard *et al.* 2003). Briefly, denatured, individual skinned fibres, or muscle sections, from SCI-S and CTL vastus lateralis were diluted in 50 mmol l^{-1} carbonate–bicarbonate buffer (pH 9.0) and placed on the bottom of a microtitrate plate. The primary antibody recognizing desmin (1 : 20; Sigma-Aldrich, Schnelldorf, Germany) was followed by an alkaline phosphatase-conjugated secondary antibody (1 : 350; chicken anti-rabbit, Santa Cruz Bioscience, Heidelberg, Germany). The plates were analysed in an ELISA reader (iEMS Reader MF, Labsystems, Finland) at optical density 405/490 nm and the desmin concentration in each fibre

was related to its total protein content as determined by a commercially available protein quantification kit (NanoOrange, N-6666, Molecular Probes, Leiden, The Netherlands).

Data analysis

All data are presented as means ± standard error of the mean (S.E.M.). Statistical analyses of the data were performed using either a repeated measures analysis of variance (ANOVA) or Student's unpaired *t* tests when appropriate, except for the comparison of MyHC isoforms determined from single fibres where the non-parametric Mann-Whitney rank sum test was used. P values < 0.05 were taken as indicating significant differences.

Results

Whole-muscle passive tension is increased in patients with spasticity

Torque recordings during passive lengthening of proximal leg muscles at four constant speeds of movement between 15 and 120 deg s^{-1} were collected from patients with spasticity and control subjects using an isokinetic dynamometer (Fig. 1). On average, torque opposing the

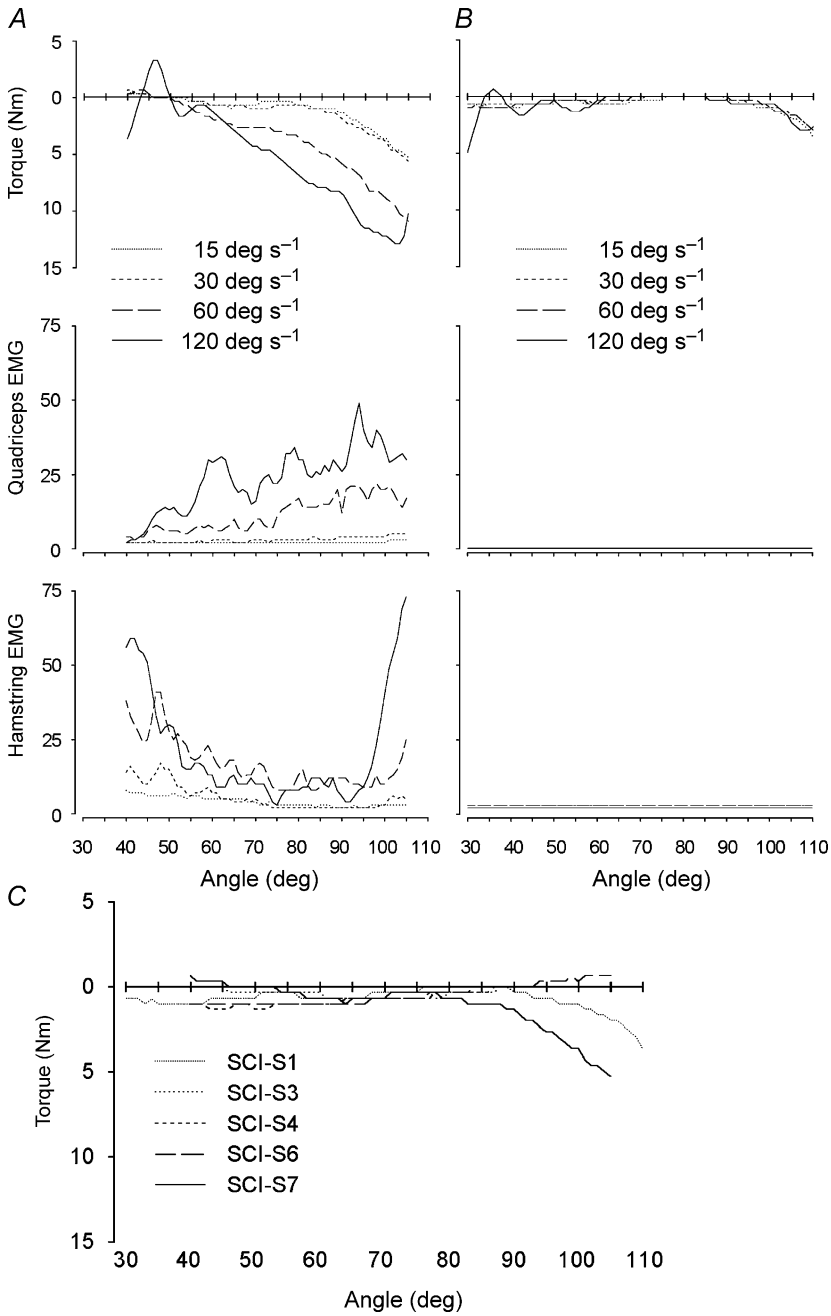

Figure 1. Passive flexion of the knee joint at four different constant angular velocities
Passive flexion in a SCI-S patient with (*A*) and without (*B*) velocity-dependent stretch reflexes. Torque curves give gravity-corrected mean torque from three repeated tests. Negative torque indicates resistance to the movement. EMG activity is given as a mean of rectified and filtered surface EMG recorded from the quadriceps and the hamstrings muscle groups. *C*, passive flexion of the knee joint at a constant angular velocity of 15 deg s^{-1} in five different SCI-S subjects. Records from two of the patients were excluded from the graph since the torque recording was dominated by factors unrelated to the quadriceps muscle, precluding interpretation of its contribution to the passive tension.

movement, along with EMG activity both in lengthened and shortened muscles, was increased for extensions and flexions at the higher speeds of movement in the SCI-S group (Fig. 1*A* and *B*). Control subjects showed no resistance to the movement and no or very low levels of muscle activation during passive movements of the limb, independent of knee angle, i.e. muscle length (data not shown). However, resistance and muscle activation varied substantially between the SCI-S patients (compare Fig. 1*A* with Fig. 1*B*). Furthermore, a significant increase in quadriceps PT was observed in some SCI-S patients at long muscle lengths (Fig. 1*C*), but never in control subjects at similar muscle lengths (not shown). The increase in PT at long muscle lengths in SCI-S was unrelated to speed of movement and muscle activation.

Single-fibre contractile properties are altered in a fibre type-dependent manner

Passive tension was increased in single skinned skeletal muscle fibres from SCI-S subjects compared with controls (ANOVA, $P < 0.01$; Fig. 2*A*). However, individual variability among fibres within the SCI-S group was large (Fig. 2*B*). Notably, the subject with the highest *in vivo* PT at long quadriceps muscle lengths (SCI-S7; Fig. 1*C*) also had the highest PT at the single-fibre level (SCI-S7; Fig. 2*B*). No difference in slack SL was found between the two groups. Moreover, maximum active force normalized to muscle fibre cross-sectional area (measured at SL 2.8 μm) was not different between the SCI-S (328 ± 27 mN mm^{-2}) and CTL (302 ± 24 mN mm^{-2}) groups, although the CSA of the single skinned fibres at SL 2.8 μm was significantly lower ($P < 0.01$) in the SCI-S ($4390 \pm 410\ \mu$m^2) than the CTL ($9550 \pm 570\ \mu$m^2) group. To account for over-estimation of single-fibre CSA due to the well-known effect of swelling of skinned muscle samples, we also measured the fibre CSA on tissue sections and obtained mean values of $3120 \pm 829\ \mu$m^2 for SCI-S and $6584 \pm 1297\ \mu$m^2 for CTL muscles (Fig. 3, inset). Thus, the fibres from spastic muscles were confirmed to be atrophic. Further, there was a much larger variability in fibre diameters in spastic than in control muscles (data not shown), which was also reflected in a large variability in fibre CSA among SCI-S muscles (Fig. 3).

For the single fibres we also established the MyHC isoform compositions (see below and Fig. 6) and then related passive tension to fibre type. Interestingly, increased PT in spasticity was found only in fibres expressing fast-type MyHC isoforms, not in those expressing slow-type MyHC (Fig. 4). Muscle fibres coexpressing types IIa and IIx MyHC showed a statistically significant difference in PT between SCI-S and CTL (Fig. 4*C*). We found only three fibres from SCI-S subjects expressing the type I MyHC isoform and no single fibres from the control group expressing the type IIx MyHC isoform, which made statistical comparisons of these isoforms difficult. Generally, muscle fibres expressing only type IIx MyHC are extremely rare in human quadriceps muscle (Larsson & Moss, 1993). However, we could obtain single muscle fibres expressing the IIx MyHC isoform unrelated to spasticity from the quadriceps muscles of track-and-field athletes (sprinters). These muscles are known to have a relatively high proportion of fast MyHC isoforms (Gur *et al.* 2003), but most fibres expressing the IIx MyHC isoform in sprinters also coexpress the IIa MyHC isoform (Andersen *et al.* 1994). Previously we identified fibres expressing the IIx MyHC isoform alone in 6 out of 17 sprint-trained track-and-field athletes (Korhonen

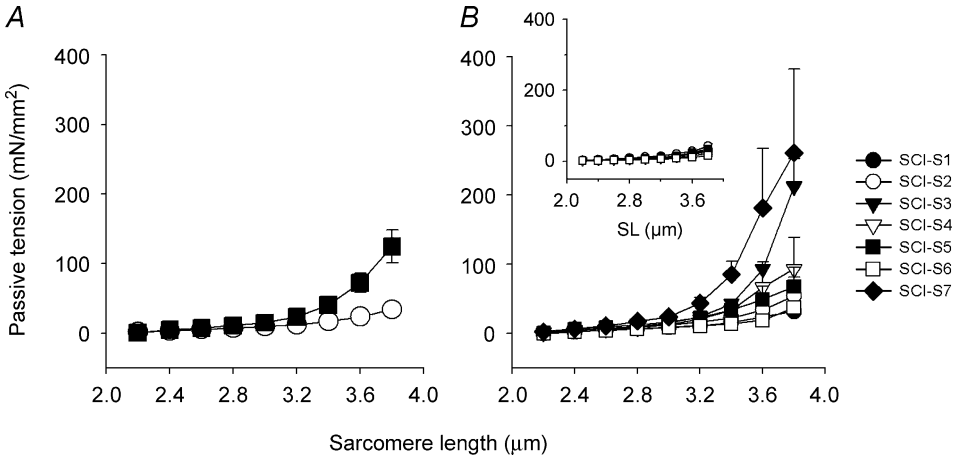

Figure 2. Single-fibre passive tension differs between controls and SCI-S patients
A, average PT *versus* sarcomere length (SL) relationships of skinned single muscle fibres. SCI-S patients, ■; control subjects, ○. *B*, high variability in PT among SCI-S subjects. Symbols represent PT measurements from individual SCI-S muscles (see key in figure). Inset: low variability in PT among control subjects, symbols represent individual CTL muscles. Data points are means ± S.E.M.

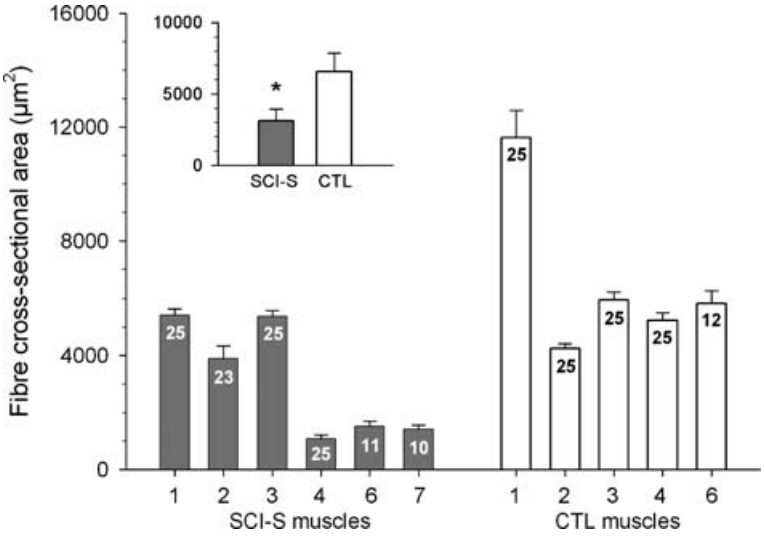

Figure 3. Cross-sectional area of single fibres from human SCI-S and CTL vastus lateralis determined by histological analysis of cross-sections
Results are shown for individual subjects; numbers in columns indicate number of single fibres measured. Inset: 'mean of means' for SCI-S and CTL muscles. Data are means ± S.E.M. * $P < 0.05$ in Student's *t* test.

et al. 2006). Here we used eight pure type IIx fibres from five sprinters to compare the PT at 2.8 μm SL with that of 16 type IIx fibres from SCI-S patients (Fig. 4*D*, inset). MyHC-IIx fibres from SCI-S had an approximately 50% higher PT than those from controls ($P < 0.05$), indicating that the increased PT was secondary to spasticity *per se*.

Myofibrillar passive tension remains unchanged in spasticity

Passive force measurements were performed on non-activated isolated myofibrils obtained from four SCI-S and three CTL patients. We used those SCI-S

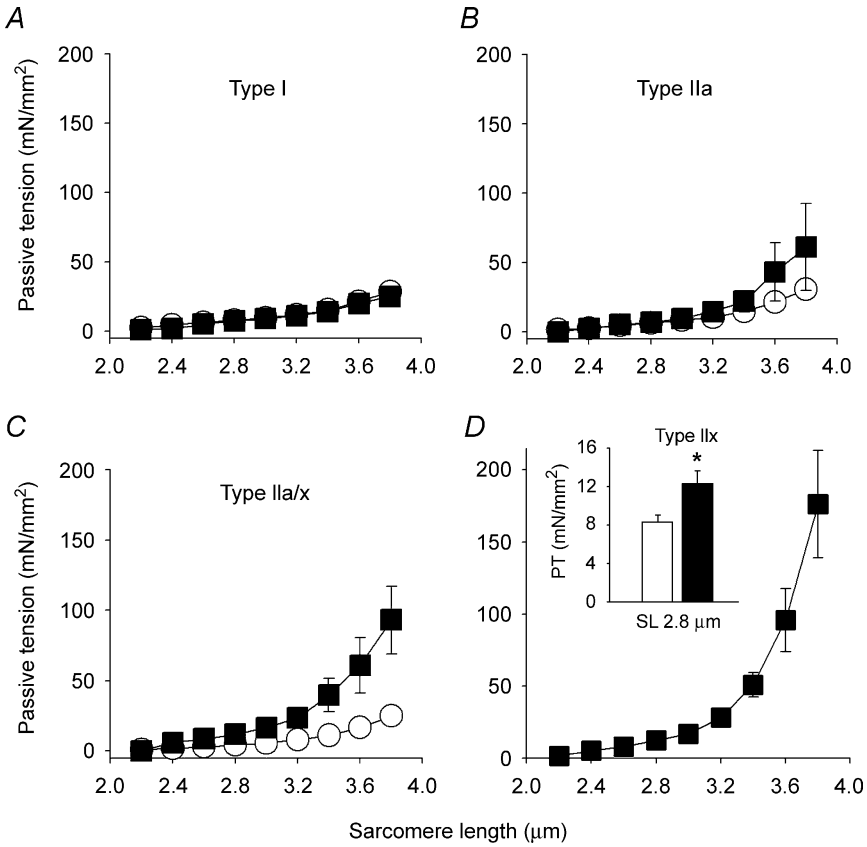

Figure 4. MyHC type-dependent passive tension increase in skinned single fibres from SCI-S patients
A, no difference in PT between SCI-S ($n = 3$) and CTL ($n = 11$) in fibres expressing type I MyHC. *B*, no statistically significant ($P > 0.05$) difference in PT between SCI-S ($n = 5$) and CTL ($n = 9$) in fibres expressing type IIa MyHC. *C*, significant differences ($P < 0.01$, at all sarcomere lengths above slack) in PT between SCI-S ($n = 6$) and CTL ($n = 8$) in fibres expressing a mix of IIa and IIx MyHC isoforms. *D*, PT was highest in type IIx MyHC fibres from SCI-S patients ($n = 16$). Inset: comparison of PT at SL 2.8 μm for IIx fibres from healthy athletes ($n = 8$, open column, otherwise not included in this study) and SCI-S patients ($n = 16$, filled column). SCI-S patients, ■; control subjects, ○. * Significantly different at $P < 0.05$. Data points are means ± S.E.M.

muscles that showed the highest PT increase at the single-fibre level (SCI-S7, 3, 4 and 5; see Fig. 2*B*). However, passive tension during stepwise stretch from SL 1.8 to 3.6 μm was not different between myofibrils from the SCI-S and CTL groups (Fig. 5). Pooled results for the individual muscles from the two groups are shown in Fig. 5*B*, indicating that none of the variability seen at the whole-muscle and single-fibre levels remains at the myofibrillar level.

MyHC isoforms, but not titin isoforms and desmin content, are altered in spastic muscles

Gel electrophoretic studies were performed on muscle homogenates as well as single fibres to establish the MyHC isoform compositions. For muscle homogenates, a representative gel is shown in Fig. 6*A*. Densitometry results for muscle homogenate gels demonstrated that the SCI-S group exhibits a significantly higher proportion of fast MyHC isoforms than the CTL group ($P < 0.05$; Fig. 6*B*). Similar results were obtained at the single-fibre level (Fig. 6*C*); the difference between SCI-S fibres and control fibres, as determined by the non-parametric Mann-Whitney rank sum test, again was statistically significant ($P < 0.01$).

Skeletal muscles contain titin isoforms varying in size between approximately 3.3 and at least 3.7 MDa (Freiburg *et al.* 2000; Prado *et al.* 2005). The titin isoform size of human vastus lateralis muscles was found to be similar (~3.7 MDa) to that of the human soleus muscle, for which the titin sequence is known (Freiburg *et al.* 2000) (Fig. 7*B*). To obtain reliable titin size values, control and SCI-S vastus lateralis muscle tissue was mixed with rabbit psoas, which expresses two titin isoforms at 3300 and 3400 kDa

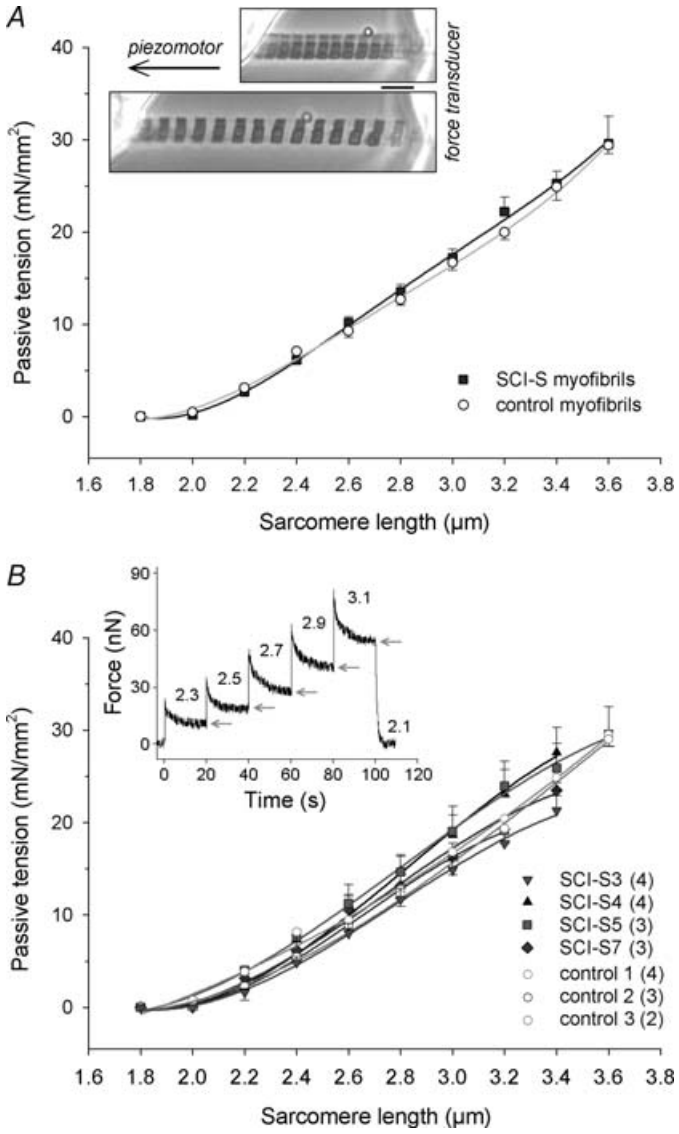

Figure 5. Passive sarcomere length–tension relationships of isolated myofibrils from human vastus lateralis
A, summary ('mean of means') showing no difference in myofibrillar passive tension between control (○; $n = 9$ myofibrils from 3 different subjects) and SCI-S (■; $n = 14$ from 4 subjects). Data points are means ± S.E.M.; fits are three-order regressions. Inserted micrograph: myofibril preparation suspended between force transducer and piezomotor and stretched from slack SL (2.0 μm) to 3.0 μm SL. Scale bar, 5 μm. *B*, myofibrillar passive tension shown for individual subjects. The number of myofibrils analysed per muscle type is indicated in the key. Data points are means ± S.E.M.; fits are three-order regressions. Inset: original force trace of a typical recording. Only quasi-steady-state force (arrows) was used for analysis. Numbers above trace indicate SL (in μm).

(Prado *et al.* 2005), and the rabbit psoas titin bands were used as internal size markers (Fig. 7*C* and *D*). However, in none of the seven SCI-S muscles was a difference in titin isoform size detectable in comparison to controls (Fig. 7). The intermuscle variability in titin size was between 3660 and 3700 kDa and the mean of seven means per group reached 3682 ± 11 kDa for the spastic muscles and 3680 ± 9 kDa for the control muscles (Fig. 7*E*). Moreover, there was no difference with regard to the stoichiometry between titin and myosin for SCI-S and CTL muscles determined from 2.8% SDS-PAGE gels (data not shown): the titin : MyHC ratio (not corrected for molecular weight) was 0.20 ± 0.03 and 0.22 ± 0.06, respectively.

The PT of single fibres is influenced not only by titin but by intermediate filaments as well. Therefore we studied the desmin protein expression levels in single fibres and whole muscle homogenates. The total protein concentration was lower in both single fibres and whole muscles in SCI-S compared to CTL ($P < 0.05$), but for the relative desmin content no statistical difference was found between patients and controls (Table 2). Furthermore, the relative desmin content of single fibres did not correlate with the MyHC isoform (data not shown).

Ultrastructural changes in spasticity involve the muscle cells and the extracellular matrix

Histological analyses (not shown) and electron micrographs (Fig. 8) prepared from vastus lateralis biopsies of SCI-S subjects demonstrated extensive remodelling compared to CTL muscles. These changes included (see Fig. 8*A*): (i) a distinct increase in collagen content and connective tissue, (ii) the presence of lipid droplets, and (iii) replacement of myofibrils by amorphous, dot-like material. Moreover, in accordance with the increased proportion of fast-twitch fibres, the average mitochondrial density in SCI-S muscles was significantly lower than in CTL muscles, $4.5 \pm 0.5\%$ *versus* $11.0 \pm 0.8\%$ (Fig. 8*Bc*). The average myofibrillar volume fraction however, remained unchanged ($80.5 \pm 2.9\%$ in control muscles; $78.6 \pm 3.1\%$ in spastic muscles) which was probably related to the (observed) relative abundance

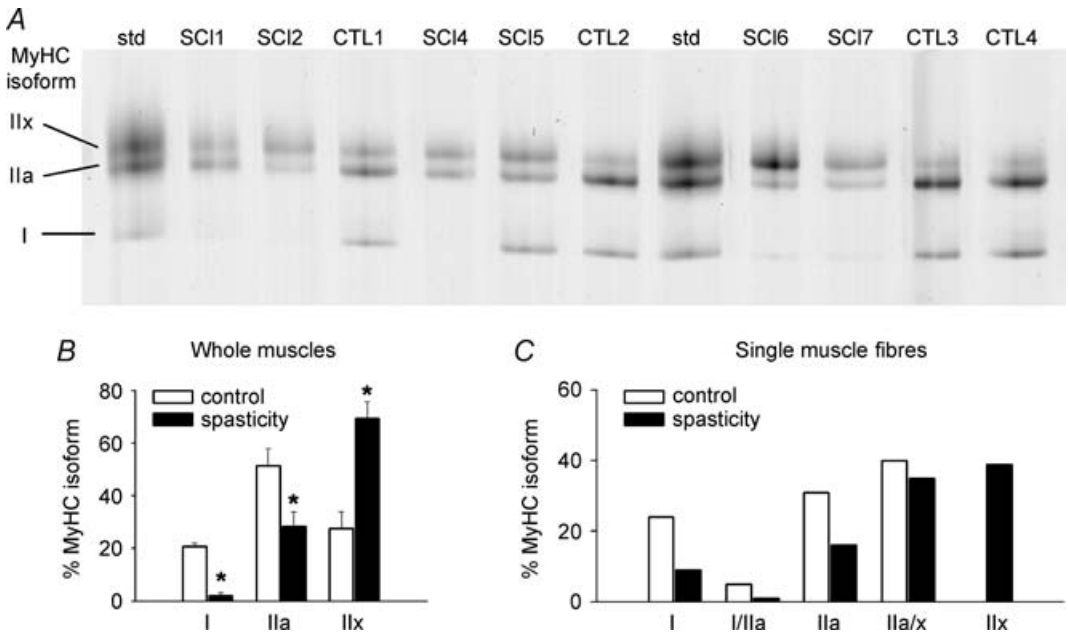

Figure 6. Myosin heavy chain isoforms in vastus lateralis biopsy samples from spinal cord-injured patients (SCI-S) and control subjects (CTL)

A, separation of MyHC isoforms (I, IIa, IIx) in muscle homogenates by 6% SDS-PAGE. SCI-S patients had less type I and more type IIx isoforms compared to CTL. Std, standard containing all three human MyHC isoforms. *B*, relative amount of MyHC isoform expression in muscle homogenates determined by densitometry on SDS-PAGE gels. Significant differences in MyHC isoform proportions were observed between the two groups ($P < 0.05$) according to ANOVA or Students' *t* test (asterisks). Data are means ± S.E.M. *C*, MyHC isoform analysis in single fibres. Shown are the percentages of individual MyHC isoforms expressed in SCI-S ($n = 138$) and control fibres ($n = 108$). The MyHC isoform percentage thus reflects fibre-type percentage. The proportion of fast MyHC isoforms was significantly increased in SCI-S fibres compared to control fibres, as determined by the non-parametric Mann-Whitney rank sum test ($P < 0.01$).

of amorphous material inside the myofibres of spastic patients.

Discussion

This study explored passive tension and spasticity in skeletal muscles from the whole muscle to the myofibrillar levels and the relation to structural and contractile protein expression in patients with an upper motor neuron lesion after spinal cord injury at the cervical or thoracic levels (SCI-S). A significant spasticity-related increase in PT was observed at the whole-muscle and single-fibre levels. We demonstrated that increased PT in SCI-S patients is associated with a higher relative content of muscle fibres expressing the type IIx MyHC isoform. Interestingly, only the fast-type fibres showed a significant increase in PT. The differences in PT between SCI-S and CTL did not persist at the myofibrillar level and were not due to changes in titin isoforms or relative desmin content. We present evidence that spasticity and increased PT are associated with major ultrastructural remodelling not only within the extracellular matrix but also inside the muscle fibres.

Patient heterogeneity

A detailed understanding of the neural and muscular mechanisms underlying the muscle hypertonus in patients with spasticity is of vital importance for the design of treatment, as some patients fail to respond to conventional treatment, e.g. botulinum toxin injections. In patients with

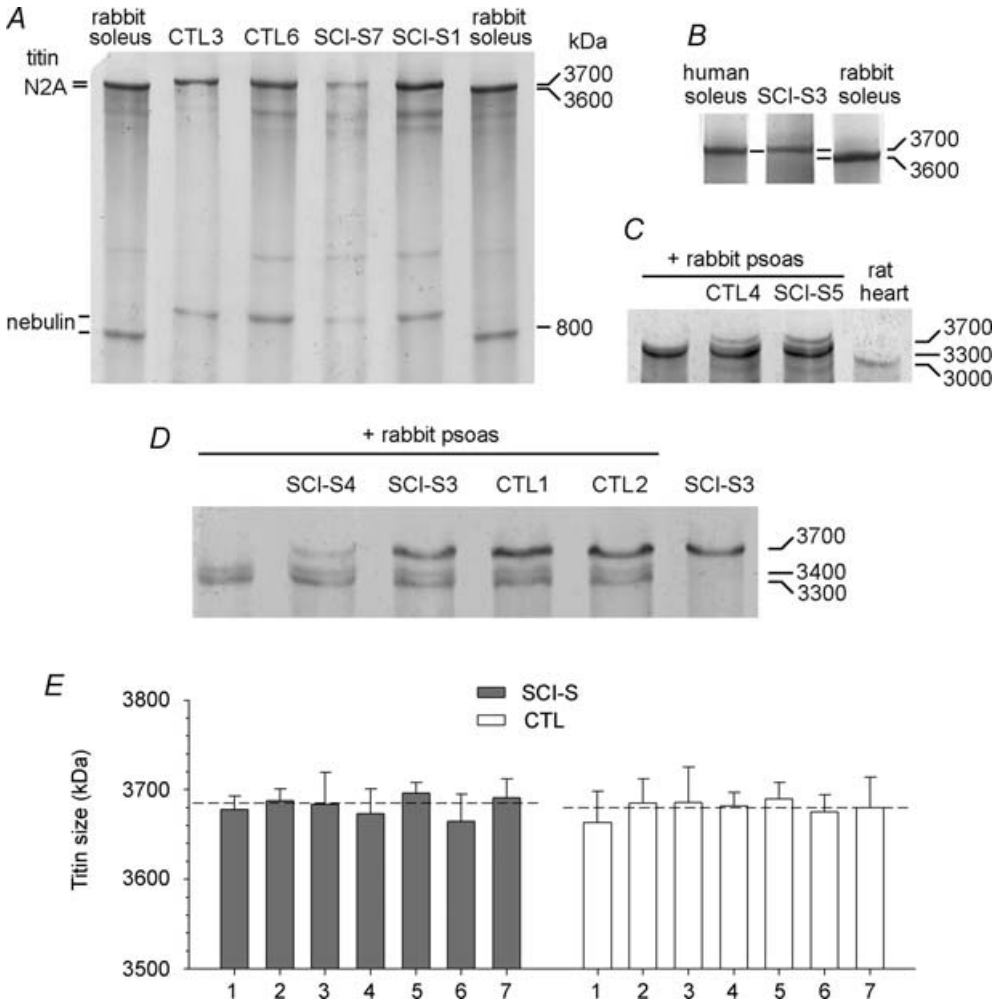

Figure 7. Titin isoform sizes in vastus lateralis biopsy samples from SCI-S and control subjects, detected by 2% SDS-PAGE
The gel electrophoretic mobility of titin was analysed in comparison to rabbit soleus (*A*; titin, ∼3600 kDa); human soleus (*B*; titin, 3700 kDa); rat heart (titin, 3000 kDa) and rabbit psoas (two titin bands at 3300 and 3400 kDa) (*C*), which was also mixed with the vastus lateralis muscle; and, again, rabbit psoas (mix) (*D*). *E*, mean values for titin size in individual muscles. Each column shows the mean ± S.E.M. measured from at least three different gels. Dashed lines indicate the 'mean of means' ($n = 7$): spastic, 3682 ± 11 kDa; control, 3680 ± 9 kDa.

Table 2. Relative desmin content and total protein concentration in the vastus lateralis whole-muscle homogenates and single fibres from SCI patients with spasticity and from control subjects

	Control	Spasticity	*P* value
Whole muscle homogenates			
Relative desmin content (desmin/total protein, %)	13.0 ± 0.5	11.1 ± 1.3	0.22
Total protein concentration (μg ml^{-1})	18.2 ± 0.4	16.8 ± 0.3	0.03
Number of muscle samples	$n = 6$	$n = 6$	
Single fibres			
Relative desmin content (desmin/total protein, %)	39.1 ± 4.1	26.9 ± 6.1	0.10
Total protein concentration (μg ml^{-1})	7.3 ± 0.3	3.8 ± 0.2	< 0.01
Number of fibres analysed	$n = 57$	$n = 56$	

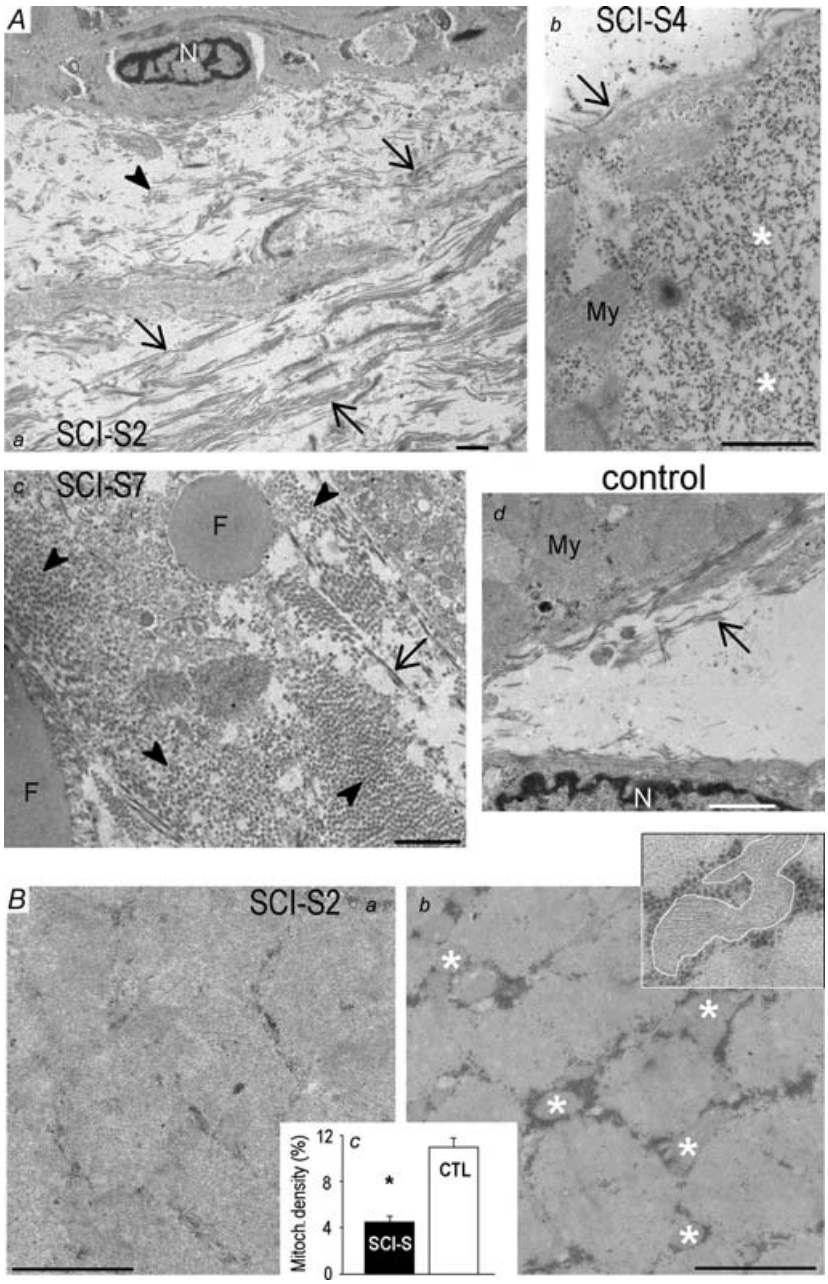

Figure 8. Ultrastructural remodelling in SCI-S muscles
A, collagen accumulation and connective tissue expansion in spasticity. Representative electron micrographs of spastic (*a*, *b* and *c*) and control (*d*) human muscles. Images of SCI-S muscles are from three different patients. Note the extensive collagen depositions (*a* and *c*), lipid droplets (*c*), and replacement of myofibrils by amorphous material (*b*, asterisks) in spasticity. Arrows, collagen fibres in longitudinal section; arrowheads, collagen in cross-section; My, myofibrils; N, nucleus; F, fat (lipid) droplets. *B*, decreased mitochondrial volume density in spasticity. Typical electron micrographs of cross-sections obtained from spastic (*a*) and control (*b*) muscles. Some of the mitochondria are highlighted by asterisks. Inset in *Bb*: higher-magnification image showing encircled mitochondria. *Bc* demonstrates average mitochondrial area percentage relative to total area on micrographs of SCI ($n = 4$ muscles, 20 images) and CTL samples ($n = 4$ muscles, 20 images). Data are means $\pm$ S.E.M. * Significantly different at $P < 0.05$. All scale bars are 1 μm.

spasticity secondary to an upper motor neuron lesion, increased PT at the whole-muscle level is a common feature (Tardieu *et al.* 1982; Sinkjaer *et al.* 1993; Mirbagheri *et al.* 2001). Indeed, some of the SCI-S patients studied here showed increased resistance to stretching of the quadriceps muscle, although other patients did not. The increased resistance to stretch, when present, was not of the same origin in different patients. In some, it was velocity dependent, increasing with increasing velocity and most likely due to exaggerated stretch reflexes. In others, it was muscle-length dependent and unrelated to muscle activity, increasing only at the end of the movement range, probably due to structural alterations. This large variability in *in vivo* PT of SCI-S patients is consistent with previous observations (Knutsson *et al.* 1997). However, we were not able to identify any clinical parameter underlying the inter-patient variability in PT, i.e. PT did not correlate with the duration of spasticity, the spinal level of the traumatic injury, age of subjects, or medication.

MyHC isoform expression and fibre-type dependence of PT increase in spasticity

Recent work has shown that increased resistance to stretch and high PT in patients with spasticity also persist at the single-fibre level (Fridén & Lieber, 2003; Lieber *et al.* 2004). Our results on skinned single fibres agree with these findings. Although no earlier study has related increases in PT to specific MyHC isoforms, previous work on patients with SCI (but unknown spasticity levels) demonstrated an increase in fast MyHC isoforms within a year of the injury (reviewed in Talmadge, 2000). Elsewhere, the muscles of SCI-S patients were found to have a higher percentage of fast MyHC isoforms than those of control subjects (Fridén & Lieber, 2003). However, there are conflicting reports as to whether there is a general MyHC isoform switch in response to spasticity, which may be related to the fact that different muscles were studied from controls and spastic patients, and that individuals in the two groups were usually of different age (reviewed in Lieber *et al.* 2004). In the present work we avoided these shortcomings and observed a significant increase in MyHC-IIx isoform expression in the SCI-S group. This fibre-type shift in spastic muscles occurred in addition to fibre atrophy, confirming previous observations. Our results thus support the notion of a shift toward fast MyHC isoforms most likely as a consequence of chronic decreased use of the spastic muscles.

A novel finding of this work is that PT in the SCI-S patients increased in a MyHC isoform-dependent manner. There was an almost 10-fold increase in PT in spastic muscle fibres expressing the type IIx isoform compared with those expressing type I MyHC (Fig. 4). In contrast, single fibres containing type IIx MyHC showed no elevated PT in muscles of healthy athletes, suggesting that higher PT of type IIx fibres in SCI-S patients represents an adaptation to the upper motor neuron lesion. In summary, the elevated PT only in fast-type fibres, together with an increased proportion of fast-type IIx fibres, contribute to the increased PT in SCI-S patients at the whole-muscle level.

Known passive tension-generating proteins in the fibres are unaltered in spastic muscles

We hypothesized that increased PT in spastic muscles is due to changes in titin isoforms since the PT of muscle fibres is closely related to titin isoform size (Wang *et al.* 1991; Horowits, 1992; Linke *et al.* 1996; Prado *et al.* 2005). Titin isoform changes have been reported, e.g. in end-stage failing human hearts (Neagoe *et al.* 2002; Makarenko *et al.* 2004). Here the titin in human vastus lateralis muscles was compared to the titin bands in rabbit psoas muscles serving as internal markers to obtain a high reliability of the titin size estimates (Prado *et al.* 2005). However, no statistically significant changes in titin isoform size were found between SCI-S and CTL. Similarly, spastic and control muscles exhibited no difference in the titin : MyHC ratio. Consistent with these results, PT was similar in the two groups at the isolated myofibril level. Notably, the values of PT in isolated myofibrils (Fig. 5), particularly at high SLs, were similar to those of slow skinned fibres, but lower than in fast skinned fibres (Fig. 4). Therefore the possibility exists that all SCI-S myofibrils studied mechanically were from slow fibres. However, our finding that there is no change in titin isoform size in spasticity patients (Fig. 7) supports our conclusion that myofibrillar PT, which has been shown to be higher, the smaller the titin isoform (Prado *et al.* 2005), remains unaltered in SCI-S muscles. Taken together these data suggest that the spasticity in SCI-S patients is not associated with a change in titin expression and titin-based stiffness.

Within the physiological SL range ($\sim$2.0–4.0 μm) titin is not the sole source of PT (Wang *et al.* 1993; Neagoe *et al.* 2003; Prado *et al.* 2005), as collagen fibres and also intermediate filaments (desmin) become important contributors to PT at longer SLs (Granzier & Wang, 1993; Wang *et al.* 1993). At these longer SLs we found the greatest spasticity-related increase in PT of single fibres. The desmin content has also been observed to differ between rat muscles in response to denervation; the protein decreased in the slow-twitch soleus muscle but increased in the fast-twitch gastrocnemius (Boudriau *et al.* 1996). Elsewhere, the PT of desmin-deficient mice reportedly increased (Anderson *et al.* 2001), decreased (Shah *et al.* 2004), or remained unchanged (Anderson *et al.* 2002). Our quantitative desmin measurements did not reveal differences in relative desmin content between

SCI-S and CTL muscles. Further, there was no correlation between relative desmin content and MyHC isoform despite the higher PT in muscle cells from the SCI-S group expressing IIx MyHC or a combination of IIa and IIx isoforms. In summary, the intracellular proteins commonly thought to contribute to PT generation in striated muscle were unaltered in the vastus lateralis from spasticity patients, thus leaving the PT of the myofibrils unaffected.

Cellular mechanisms of passive stiffening in spasticity

In the absence of changes in titin and desmin expression and in titin-based stiffness, the increased PT in single fibres from SCI patients with spasticity appears to be somehow associated with the shift toward the faster MyHC isoforms (IIx alone or in combination with IIa MyHC). Consistent with the higher frequency of fast-type fibres, muscles from the SCI-S group showed decreased mitochondrial volume density, but there was no concomitant increase in the myofibrillar volume fraction of spastic muscle fibres (and no change in active tension), as some myofibrils were apparently replaced by amorphous material. If this material were stiffer than the myofibrils, its presence could add to the increased PT in spastic fibres. Further along this line, we speculate that the myofibrils in fast-type fibres of spastic muscles may be particularly vulnerable to replacement by such amorphous material, which would be an explanation for the elevated PT in these fibres. Fast-type fibres appear to be more susceptible than slow fibres to external force-induced microtraumatic damage, even in healthy subjects (Fridén *et al.* 1983) and this predisposition may be aggravated in spastic muscles, perhaps leading to increased remodelling inside the fast fibres. Finally, Fridén & Lieber (2003) suggested that the collagen content could be increased even at the single 'demembranated' fibre level where theoretically no collagen should remain, and this might explain increased PT. Whether there were collagen remnants in our study was not determined, but the fact that we found MyHC isoform-specific changes in PT speaks against some generally increased presence of collagen around the muscle fibres.

In conclusion, although the primary lesion in spinal cord-injured patients with spasticity is neural in origin, profound secondary changes occur in the musculature itself at the protein, single-fibre and whole-muscle levels. The ultrastructural remodelling in spastic myocytes includes expression shifts toward increased proportions of the fast MyHC-IIx isoform, in association with elevated passive tension only in these fast-type fibres, although titin size and titin-based stiffness remain unaltered. Our results extend current knowledge about muscle hypertonia and spinal cord lesions as a prerequisite for future intervention and rehabilitation strategies for patients with an upper motor neuron lesion.

References

Andersen JL, Klitgaard H & Saltin B (1994). Myosin heavy chain isoforms in single fibres from m. vastus lateralis of sprinters: influence of training. *Acta Physiol Scand* **151**, 135–142.

Anderson J, Joumaa V, Stevens L, Neagoe C, Li Z, Mounier Y, Linke WA & Goubel F (2002). Passive stiffness changes in soleus muscles from desmin knockout mice are not due to titin modifications. *Pflugers Arch* **444**, 771–776.

Anderson J, Li Z & Goubel F (2001). Passive stiffness is increased in soleus muscle of desmin knockout mouse. *Muscle Nerve* **24**, 1090–1092.

Ashworth B (1964). Preliminary trial of arisoprodol in multiple sclerosis. *Practitioner* **192**, 540–542.

Berggard C, Damberg M & Oreland L (2003). Chronic citalopram treatment induces time-dependent changes in the expression and DNA-binding activity of transcription factor AP-2 in rat brain. *Eur Neuropsychopharmacol* **13**, 11–17.

Bohannon RW & Smith MB (1987). Interrater reliability of a modified Ashworth scale of muscle spasticity. *Phys Ther* **67**, 206–207.

Boudriau S, Cote CH, Vincent M, Houle P, Tremblay RR & Rogers PA (1996). Remodeling of the cytoskeletal lattice in denervated skeletal muscle. *Muscle Nerve* **19**, 1383–1390.

Freiburg A, Trombitas K, Hell W, Cazorla O, Fougerousse F, Centner T, Kolmerer B, Witt C, Beckmann JS, Gregorio CC, Granzier H & Labeit S (2000). Series of exon-skipping events in the elastic spring region of titin as the structural basis for myofibrillar elastic diversity. *Circ Res* **86**, 1114–1121.

Fridén J & Lieber RL (2003). Spastic muscle cells are shorter and stiffer than normal cells. *Muscle Nerve* **27**, 157–164.

Fridén J, Sjöström M & Ekblom B (1983). Myofibrillar damage following intense eccentric exercise in man. *Int J Sports Med* **4**, 170–176.

Frontera WR & Larsson L (1997). Contractile studies of single human skeletal muscle fibers: a comparison of different muscles, permeabilization procedures, and storage techniques. *Muscle Nerve* **20**, 948–952.

Gajdosik RL (2001). Passive extensibility of skeletal muscle: review of the literature with clinical implications. *Clin Biomech (Bristol, Avon)* **16**, 87–101.

Granzier H & Labeit S (2002). Cardiac titin: an adjustable multi-functional spring. *J Physiol* **541**, 335–342.

Granzier HL & Wang K (1993). Passive tension and stiffness of vertebrate skeletal and insect flight muscles: the contribution of weak cross-bridges and elastic filaments. *Biophys J* **65**, 2141–2159.

Gur H, Gransberg L, vanDyke D, Knutsson E & Larsson L (2003). Relationship between in vivo muscle force at different speeds of isokinetic movements and myosin isoform expression in men and women. *Eur J Appl Physiol* **88**, 487–496.

Hackman P, Vihola A, Haravuori H, Marchand S, Sarparanta J, De Seze J, Labeit S, Witt C, Peltonen L, Richard I & Udd B (2002). Tibial muscular dystrophy is a titinopathy caused by mutations in TTN, the gene encoding the giant skeletal-muscle protein titin. *Am J Hum Genet* **71**, 492–500.

Hornby TG, Kahn JH, Wu M & Schmit BD (2006). Temporal facilitation of spastic stretch reflexes following human spinal cord injury. *J Physiol* **571**, 593–604.

Horowits R (1992). Passive force generation and titin isoforms in mammalian skeletal muscle. *Biophys J* **61**, 392–398.

Knutsson E, Martensson A & Gransberg L (1997). Influences of muscle stretch reflexes on voluntary, velocity-controlled movements in spastic paraparesis. *Brain* **120**, 1621–1633.

Korhonen MT, Cristea A, Alén M, Häkkinen K, Sipila S, Mero A, Viitasalo JT, Larsson L & Suominen H (2006). Aging, muscle fiber type and contractile function in elite sprint-trained athletes. *J Appl Physiol* **101**, 906–917.

Lange S, Xiang F, Yakovenko A, Vihola A, Hackman P, Rostkova E, Kristensen J, Brandmeier B, Franzen G, Hedberg B, Gunnarsson LG, Hughes SM, Marchand S, Sejersen T, Richard I, Edstrom L, Ehler E, Udd B & Gautel M (2005). The kinase domain of titin controls muscle gene expression and protein turnover. *Science* **308**, 1599–1603.

Larsson L & Moss RL (1993). Maximum velocity of shortening in relation to myosin isoform composition in single fibres from human skeletal muscles. *J Physiol* **472**, 595–614.

Lieber RL, Runesson E, Einarsson F & Fridén J (2003). Inferior mechanical properties of spastic muscle bundles due to hypertrophic but compromised extracellular matrix material. *Muscle Nerve* **28**, 464–471.

Lieber RL, Steinman S, Barash IA & Chambers H (2004). Structural and functional changes in spastic skeletal muscle. *Muscle Nerve* **29**, 615–627.

Linke WA, Ivemeyer M, Olivieri N, Kolmerer B, Ruegg JC & Labeit S (1996). Towards a molecular understanding of the elasticity of titin. *J Mol Biol* **261**, 62–71.

Linke WA, Popov VI & Pollack GH (1994). Passive and active tension in single cardiac myofibrils. *Biophys J* **67**, 782–792.

Makarenko I, Opitz CA, Leake MC, Neagoe C, Kulke M, Gwathmey JK, del Monte F, Hajjar RJ & Linke WA (2004). Passive stiffness changes caused by upregulation of compliant titin isoforms in human dilated cardiomyopathy hearts. *Circ Res* **95**, 708–716.

Minajeva A, Kulke M, Fernandez JM & Linke WA (2001). Unfolding of titin domains explains the viscoelastic behavior of skeletal myofibrils. *Biophys J* **80**, 1442–1451.

Minajeva A, Neagoe C, Kulke M & Linke WA (2002). Titin-based contribution to shortening velocity of rabbit skeletal myofibrils. *J Physiol* **540**, 177–188.

Mirbagheri MM, Barbeau H, Ladouceur M & Kearney RE (2001). Intrinsic and reflex stiffness in normal and spastic, spinal cord injured subjects. *Exp Brain Res* **141**, 446–459.

Moss RL, Swinford AE & Greaser ML (1983). Alterations in the Ca^{2+} sensitivity of tension development by single skeletal muscle fibers at stretched lengths. *Biophys J* **43**, 115–119.

Mutungi G & Ranatunga KW (1996). The viscous, viscoelastic and elastic characteristics of resting fast and slow mammalian (rat) muscle fibres. *J Physiol* **496**, 827–836.

Neagoe C, Kulke M, del Monte F, Gwathmey JK, de Tombe PP, Hajjar RJ & Linke WA (2002). Titin isoform switch in ischemic human heart disease. *Circulation* **106**, 1333–1341.

Neagoe C, Opitz CA, Makarenko I & Linke WA (2003). Gigantic variety: expression patterns of titin isoforms in striated muscles and consequences for myofibrillar passive stiffness. *J Muscle Res Cell Motil* **24**, 175–189.

Opitz CA, Leake MC, Makarenko I, Benes V & Linke WA (2004). Developmentally regulated switching of titin size alters myofibrillar stiffness in the perinatal heart. *Circ Res* **94**, 967–975.

Prado L, Makarenko I, Andresen C, Krüger M, Opitz CA & Linke WA (2005). Isoform diversity of giant proteins in relation to passive and active contractile properties of rabbit skeletal muscles. *J Gen Physiol* **126**, 461–480.

Shah SB, Davis J, Weisleder N, Kostavassili I, McCulloch AD, Ralston E, Capetanaki Y & Lieber RL (2004). Structural and functional roles of desmin in mouse skeletal muscle during passive deformation. *Biophys J* **86**, 2993–3008.

Sinkjaer T, Toft E, Larsen K, Andreassen S & Hansen HJ (1993). Non-reflex and reflex mediated ankle joint stiffness in multiple sclerosis patients with spasticity. *Muscle Nerve* **16**, 69–76.

Talmadge RJ (2000). Myosin heavy chain isoform expression following reduced neuro-muscular activity: potential regulatory mechanisms. *Muscle Nerve* **23**, 661–679.

Tardieu C, Huet de la Tour E, Bret MD & Tardieu G (1982). Muscle hypoextensibility in children with cerebral palsy. I. Clinical and experimental observations. *Arch Phys Med Rehabil* **63**, 97–102.

Tkatchenko AV, Pietu G, Cros N, Gannoun-Zaki L, Auffray C, Leger JJ & Dechesne CA (2001). Identification of altered gene expression in skeletal muscles from Duchenne muscular dystrophy patients. *Neuromuscul Disord* **11**, 269–277.

Udd B, Vihola A, Sarparanta J, Richard I & Hackman P (2005). Titinopathies and extension of the M-line mutation phenotype beyond distal myopathy and LGMD2J. *Neurology* **64**, 636–642.

Wang K, McCarter R, Wright J, Beverly J & Ramirez-Mitchell R (1991). Regulation of skeletal muscle stiffness and elasticity by titin isoforms: a test of the segmental extension model of resting tension. *Proc Natl Acad Sci U S A* **88**, 7101–7105.

Wang K, McCarter R, Wright J, Beverly J & Ramirez-Mitchell R (1993). Viscoelasticity of the sarcomere matrix of skeletal muscles. The titin-myosin composite filament is a dual-stage molecular spring. *Biophys J* **64**, 1161–1177.

Acknowledgements

This work was supported by grants from Linnestiftelsen för Medicinsk Forskning, Uppsala, Sweden (to M. C. Olsson), the National Institutes of Health (AR45627, AR47318, AG14731 to L. Larsson), the Swedish Research Council (8651 to L. Larsson), and the German Research Foundation (Li690/6-2 and SFB 629 to W. A. Linke). Special thanks to Yvette Hedström, Helena Svahn, and Rita Hassenrück for excellent technical assistance and to Alexander Cristea for the IIx MyHC fibre passive tension measurements.

Author's present address

M. C. Olsson: Department of Sports & Exercise Science, Malmö University, 205 06 Malmö, Sweden.